SUPPLEMENTARY INFORMATION

VISUALIZING ALTERNATIVE MRNA SPLICING IN LIVE MAMMALIAN CELLS WITH THE RIBOGLOW-FLIM SENSOR

Nadia Sarfraz[1,+], Bindu Modi[1,+], Ameeta Sihota[1], Zachary Stickelman[1], Luke K. Shafik[1], Esther Braselmann[1]*

1 Department of Chemistry, Georgetown University, Washington, District of Columbia, USA

+ These authors contributed equally
*Corresponding author
esther.braselmann@georgetown.edu

a

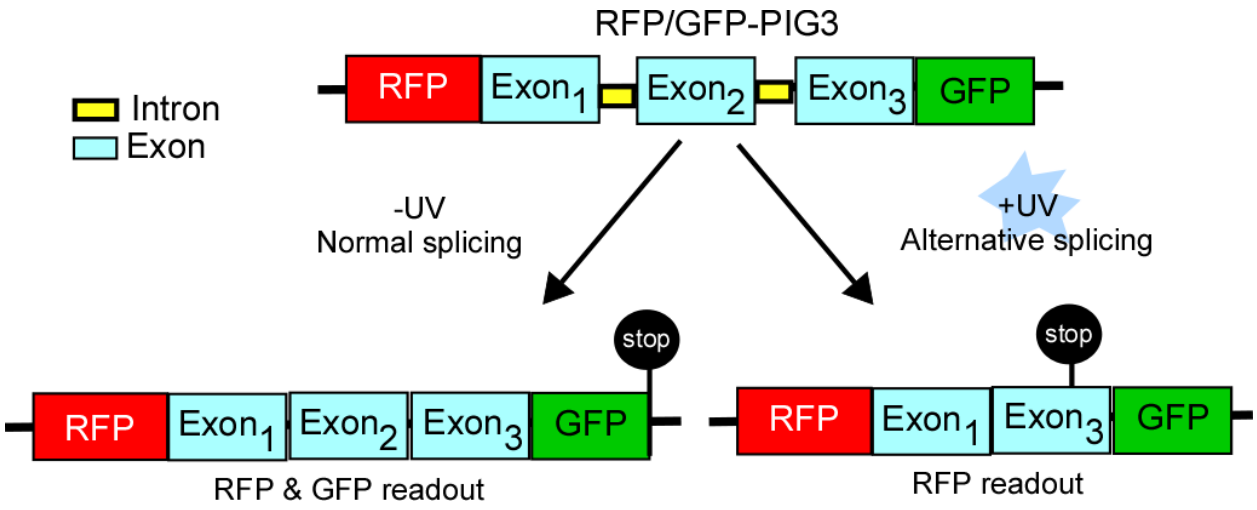

b

	Condition	Normal splice isoform	Alternative splice isoform
Gurskaya et al. (2016)[1]	HEK 293 T cells; RFP/GFP-PIG3 + UV	27 %	73 %
This study	HeLa cells; Halotag-JF/GFP-PIG3 + UV	19 ± 8%	81 ± 8%
	HeLa cells; Cntrl-RiboxPIG3	13 ± 14%	87 ± 14%
	HeLa cells; RiboxPIG3 +UV	10 ± 7%	90 ± 8%

Supplementary Figure 1. (a) Schematic of previously developed RFP/GFP-PIG3[1] system with RFP and GFP-coding regions. Splicing results in two mRNA isoforms, either a normal full-length transcript (left) producing RFP and GFP or an alternative short transcript (right) resulting in RFP only. (b) Comparison of normal and alternative transcripts produced under listed conditions. Splice isoforms were quantified by FACS analysis in Gurskaya et al, and by cell-by-cell quantification of reporter fluorescent protein signal (this study).

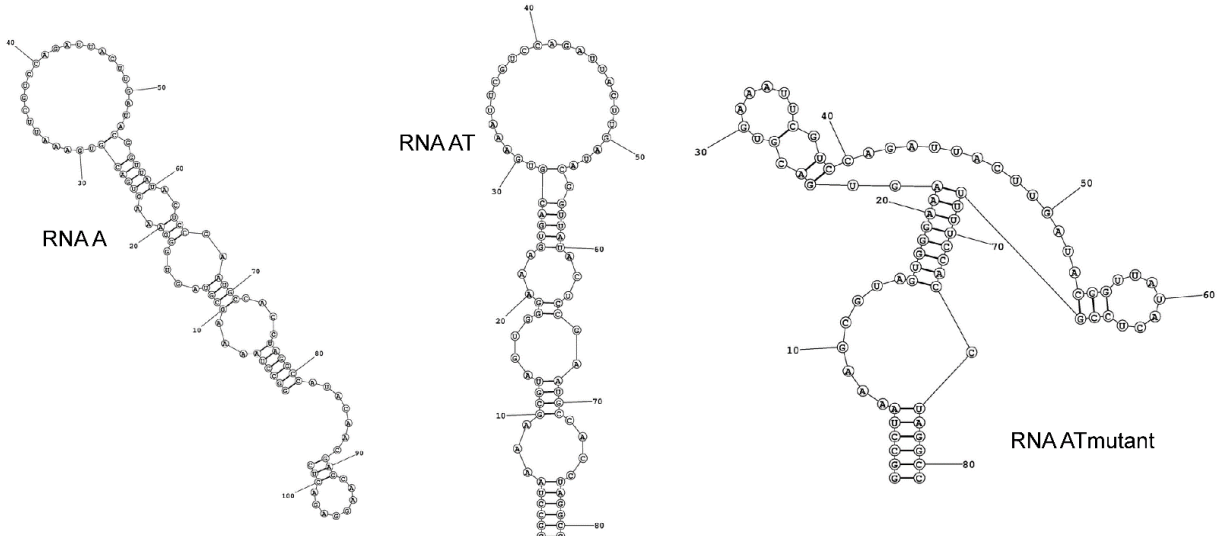

Supplementary Figure 2. MaxExpect[2] secondary structure prediction of RNA A, RNA AT, and RNA ATmutant.

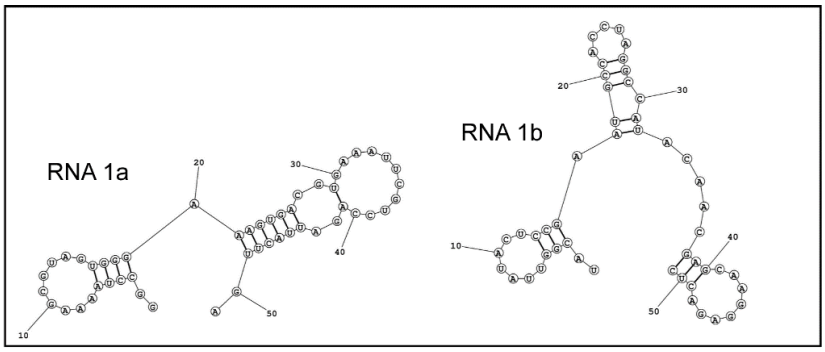
RNA 1a
RNA 1b

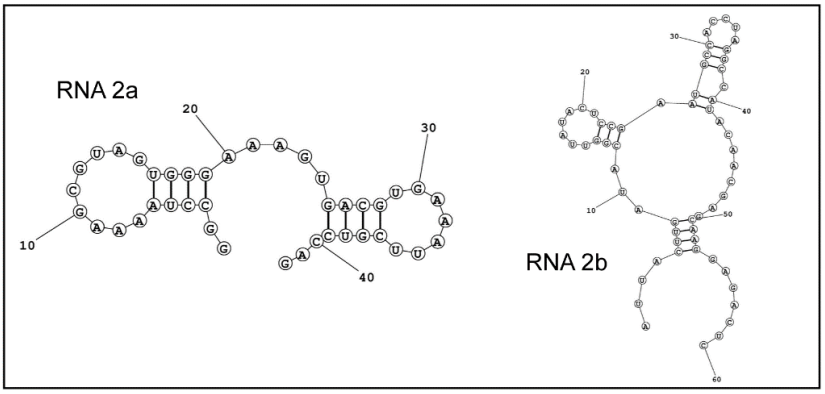
RNA 2a
RNA 2b

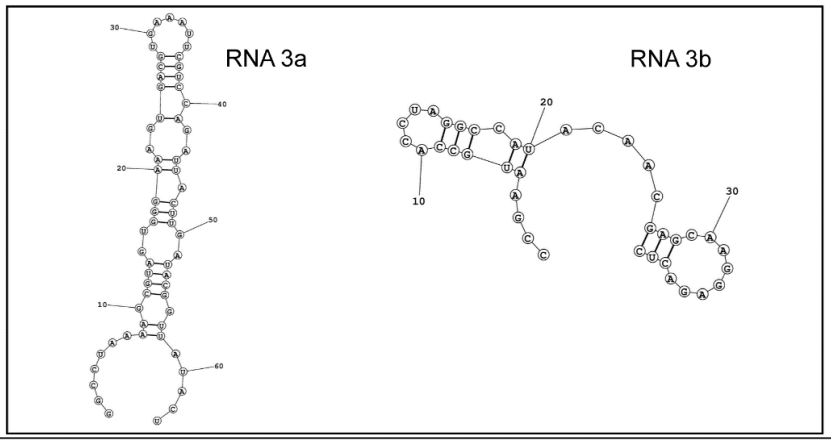
RNA 3a
RNA 3b

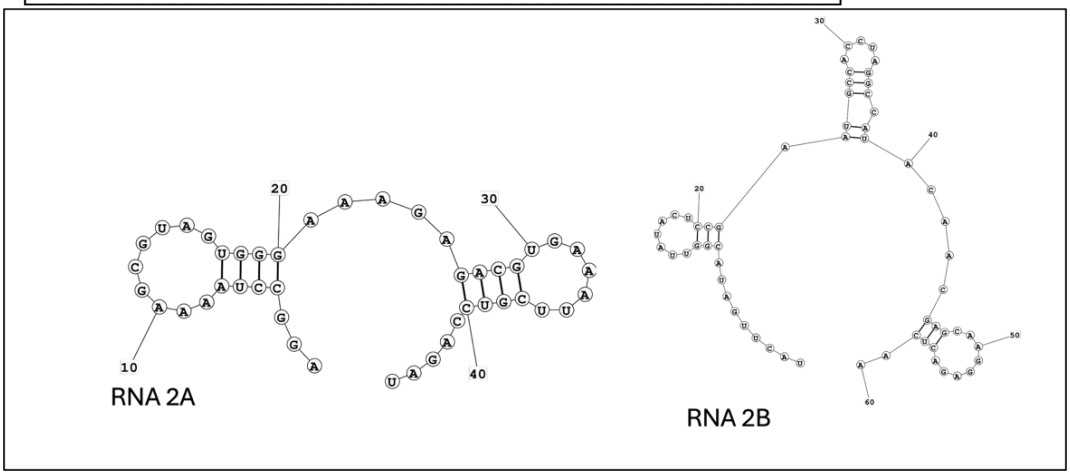
RNA 2A
RNA 2B

Supplementary Figure 3. MaxExpect[2] secondary structure prediction of split variant candidates of RNA A tag for in vitro FLIM screen.

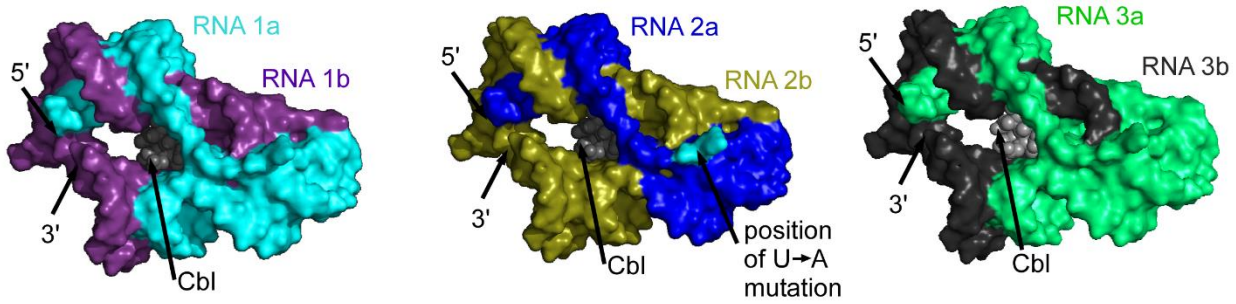

Supplementary Figure 4. Crystal structure of RNA A tag (PDB: 4FRN)[3] relative to variants designed in this study. The ligand Cobalamin is shown in grey. Color coded regions of RNA "halves" in RNA split variants 1a, 1b, 2a, 2b, 3a, 3b. For split half 2a (see also Fig. 2a for halves 2a and 2b), the position of a U→A point mutation to circumvent a premature UGA stop codon in the reading frame when incorporated in the splicing sensor is shown. Split variant 2a with that U→A point mutation is referred to as variant 2A (Figure 4). Sequences of split haves are listed in Supplementary Table 1.

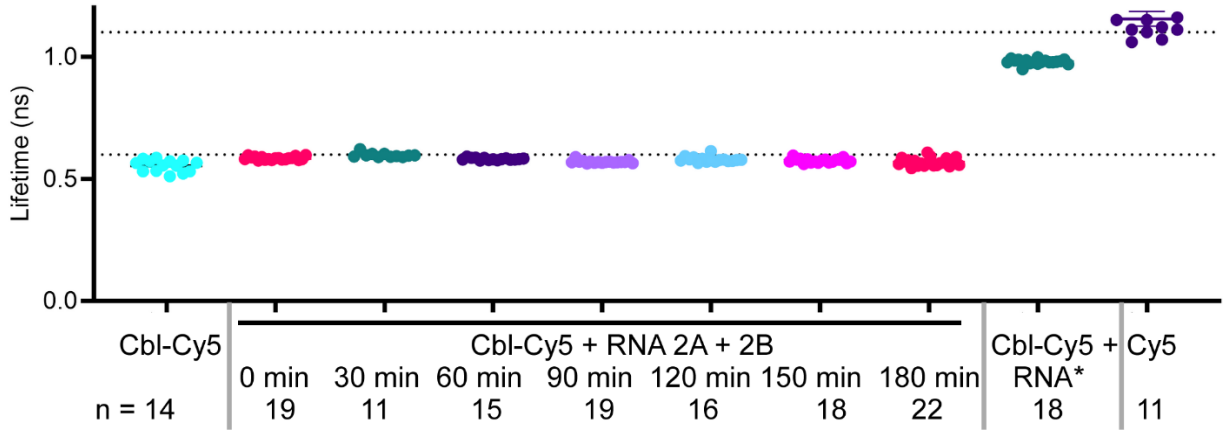

Supplementary Figure 5. Determining split tag variant fluorescence lifetime imaging microscopy (FLIM) turn-on in vitro over time in the presence Cbl-Cy5 probe after mixing split pieces. Average fluorescence lifetime values of split variants incubated together over time relative to the full A-tag (variant A*) and free Cy5 (Cy5) and Cbl-Cy5 (<4 independent experiments, data processed by multiexponential reconvolution as outlined in methods). One symbol = 1 independent experiment.

Supplementary Figure 6. Exposure of live HeLa cells transfected with reporter plasmids to continuous UV light in cell culture incubator.

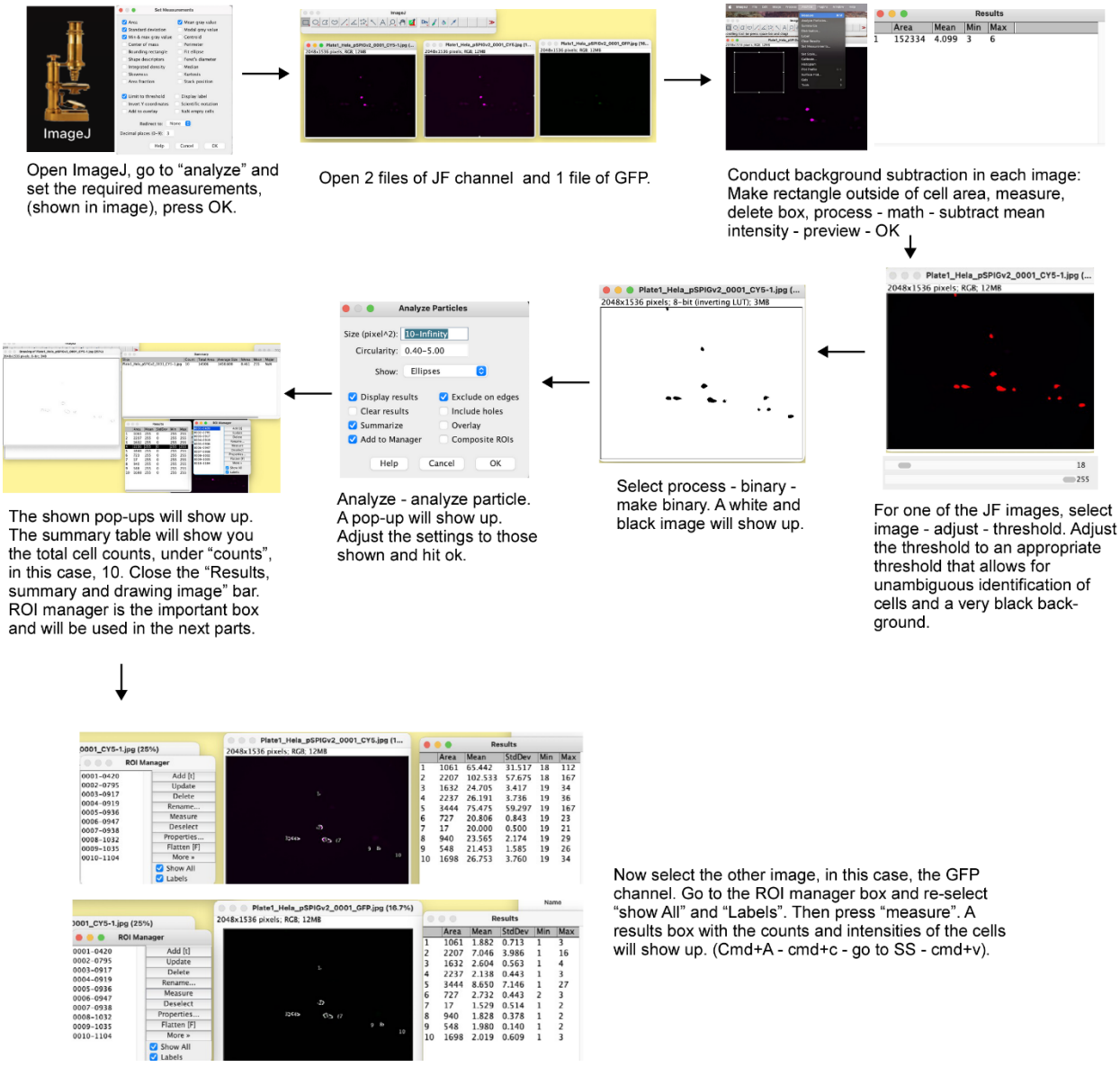

Supplementary Figure 7. Step-by-step flowchart to quantify cell-by-cell fluorescence intensity of reporter fluorescence proteins by ImageJ. Datasets were blinded before analysis.

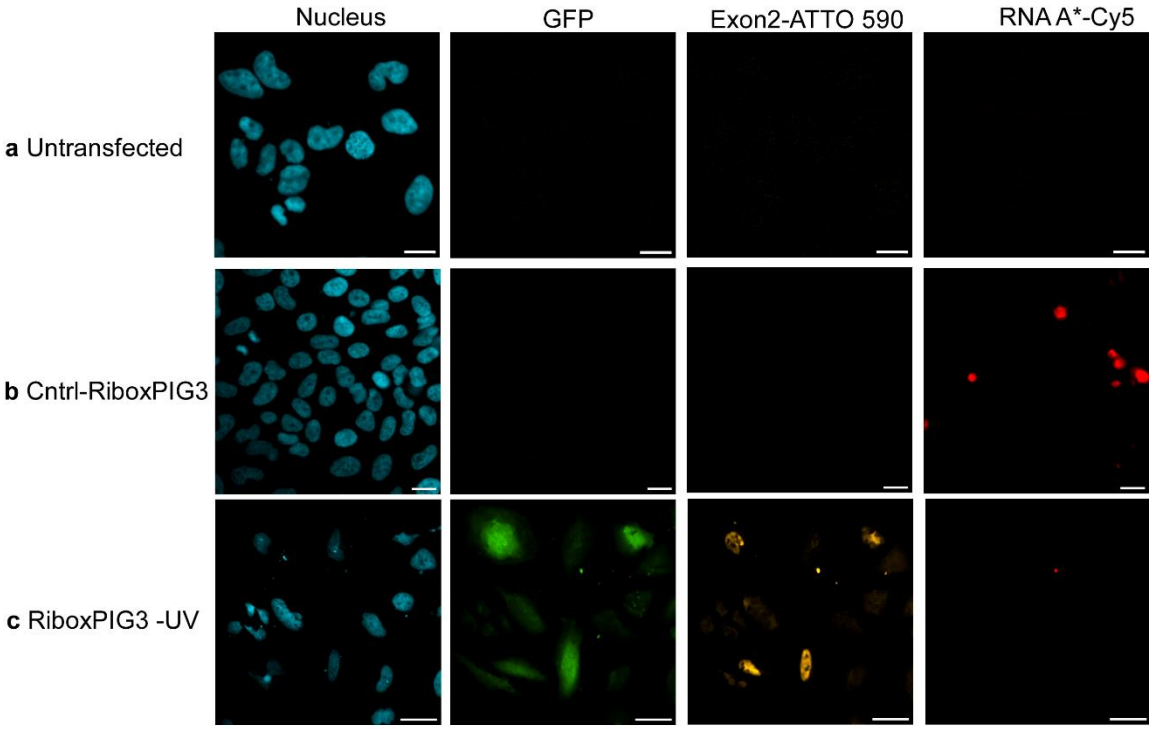

Supplementary Figure 8: Evaluation of transcripts produced in HeLa cells after transfection of plasmids to produce indicated transcripts. Cells were transfected as for live cell experiments, fixed, and the produced transcripts were assessed by the indicated FISH probes. FISH was performed with a probe targeting exon-2 (Exon2-ATTO 590), and a probe targeting the split A-tag junction (RNA A*-Cy5). Images were acquired by using a Nikon Eclipse Ti2 inverted microscope. (a) Untransfected HeLa cells (2 experiment, 343 cells) with FISH probe Exon-ATTO 590 and RNA A*-Cy5); (b) HeLa cells transfected with the Cntl-RiboxPIG3 construct with a FISH probe targeting Exon2-ATTO 590 and RNA A*-Cy5 (3 experiment, >100 cells), (c) HeLa cells transfected with RiboxPIG3-UV construct with a FISH probe Exon2-ATTO590 and RNA A*-Cy5) (1 experiment, >100 cells). DAPI was used for nuclear staining. Scale bar = 20µm.

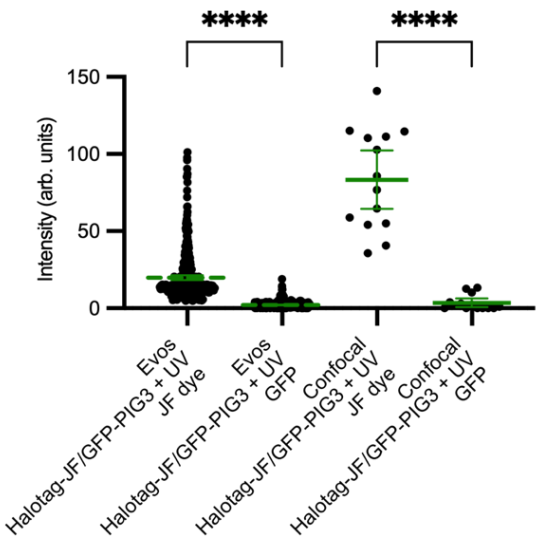

Supplementary Figure 9. Cell-by-cell fluorescence intensity of whole HeLa cells transfected with Halotag-JF/GFP-PIG3 exposed to UV or not, and illuminated by widefield or confocal microscopy. Individual intensity (1 dot = 1 cell) of each cell was measured for. Intensity of whole-cell in both GFP and Halotag-JF channel were analyzed per the ImageJ workflow in Supplementary Figure 7. HeLa cells producing fluorescent reporters were analyzed by widefield microscopy (EVOS microscope, with GFP LED light cube and EVOS Texas Red 2.0 LED Light Cube with 20x air objective) or confocal microscopy and exposed to UV light as outlined in methods (Abberrior STED confocal microscope, excitation of 594 nm (for Halotag) and 493 nm (for GFP), 20x air objective. Average GFP an Halotag-JF dye intensity of each condition was plotted. One symbol = 1 cell intensity, 2 independent experiments, > 15 cells. p-values listed (ns: $p \leq 0.5$; *$p \leq 0.05$; **$p \leq 0.01$; ***$p \leq 0.001$; ****$p \leq 0.0001$). One-way ANOVA (95% confidence limit); post hoc test (Tukey HSD).

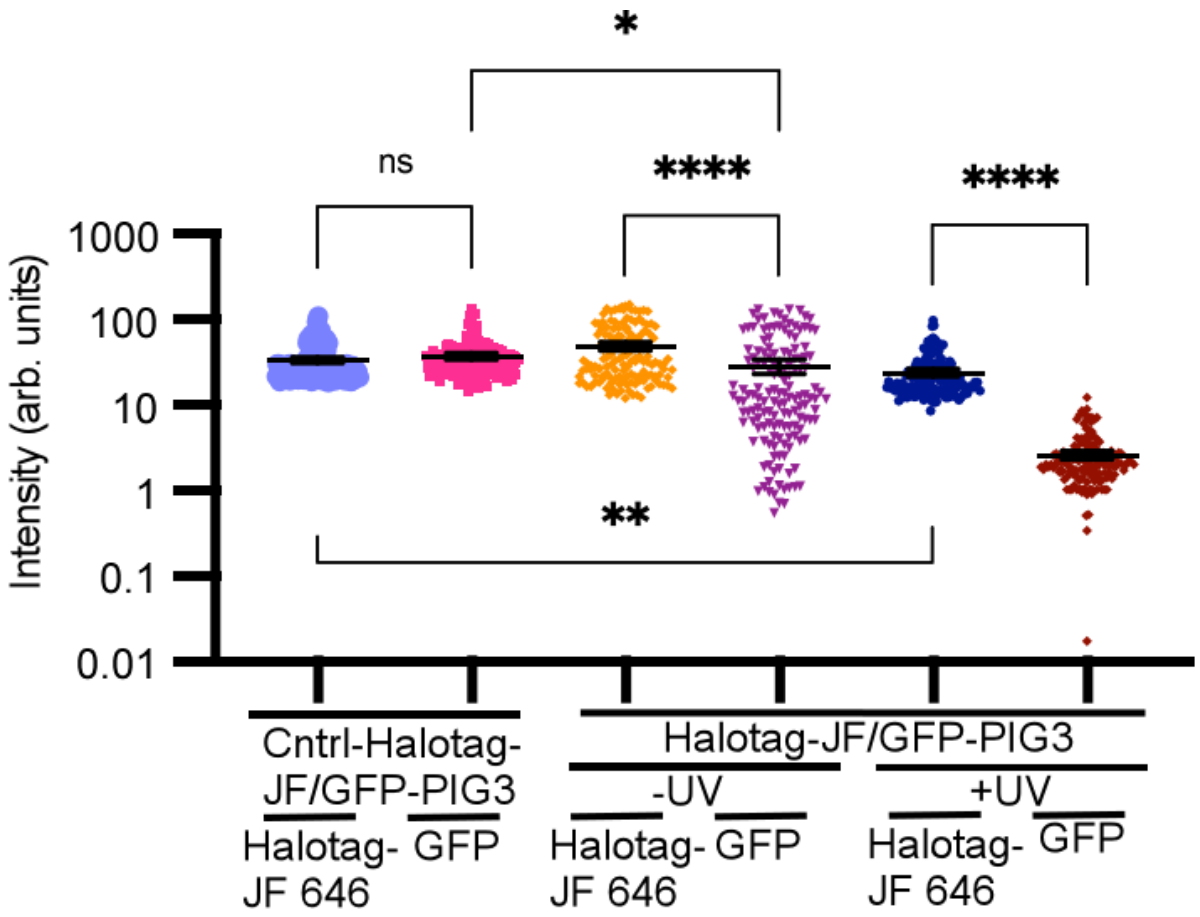

Supplementary Figure 10. Cell-by-cell fluorescence intensity of whole HeLa cells transfected with either Cntrl-Halotag-JF/GFP-PIG3 or Halotag-JF/GFP-PIG3 reporter. Individual intensity (1 dot = 1 cell) of each cell was measured outlined in the ImageJ cell fluorescence quantification workflow (Supplementary Figure 7), p-values listed (ns: $p \leq 0.5$; *$p \leq 0.05$; **$p \leq 0.01$; ***$p \leq 0.001$; ****$p \leq 0.0001$). One-way ANOVA (95% confidence limit); post hoc test (Tukey HSD).

Supplementary Table 1: Sequences of Riboglow RNA tags used in this study. RNA A tag sequence was previously reported.[5,7]

RNA Sample	Sequence
RNA A	5′-GGC CUA AAA GCG UAG UGG GAA AGU GAC GUG AAA UUC GUC CAG AUU ACU UGA UAC GGU UAU ACU CCG AAU GCC ACC UAG GCC AUA CAA CGA GCA AGG AGA CUC-3′
RNA A* (changes vs. RNA A underlined)	5′AGG CCU AAA AGC GUA GUG GGA AAG AGA CGU GAA AUU CGU CCA GAU UAC UUG AUA CGG UUA UAC UCC GAA UGC CAC CUA GGC CAU ACA ACG AGC AAG GAG ACU CAA-3′
RNA AT	5′-GGC CUA AAA GCG UAG UGG GAA AGU GAC GUG AAA UUC GUC CAG AUU ACU UGA UAC GGU UAU ACU CCG AAU GCC ACC UAG GCC-3′
RNA ATmutant (changes vs. RNA AT underlined)	5′-GGC CUA AAA GCG UAG UGG GAA AGU GAC GUG AAA UUC GUC CAG AUU ACU UGA UAC GGU UAU ACU CCG UUU UCC ACC UAG GCC-3′
RNA 1a	5′-GGC CUA AAA GCG UAG UGG GAA AGU GAC GUG AAA UUC GUC CAG AUU ACU UGA-3′
RNA 1b	5′-UAC GGU UAU ACU CCG AAU GCC ACC UAG GCC AUA CAA CGA GCA AGG AGA CUC-3′
RNA 2a	5′-GGC CUA AAA GCG UAG UGG GAA AGU GAC GUG AAA UUC GUC CAG-3′
RNA 2b	5′-AUU ACU UGA UAC GGU UAU ACU CCG AAU GCC ACC UAG GCC AUA CAA CGA GCA AGG AGA CUC-3′
RNA 2A	5′-AGG CCU AAA AGC GUA GUG GGA AAG AGA CGU GAA AUU CGU CCA GAU-3′
translated 2A (N→C)	-RPKSVVGKRREIRPD-
RNA 2B	5′- UAC UUG AUA CGG UUA UAC UCC GAA UGC CAC CUA GGC CAU ACA ACG AGC AAG GAG ACU CAA-3′
Translated 2B (N→C)	-YLIRLYSECHLGHTTSKETQ-
RNA 3a	5′-GGC CUA AAA GCG UAG UGG GAA AGU GAC GUG AAA UUC GUC CAG AUU ACU UGA UAC GGU UAU ACU-3′
RNA 3b	5′-CCG AAU GCC ACC UAG GCC AUA CAA CGA GCA AGG AGA CUC-3′

Supplementary Table 2: DNA sequences used in this study. See Fig. 3 for organization of reporter construct, Supplementary Note for alternative splicing details. Sequences of GFP[1] and Halotag[8] were previously reported. See Supp. Note 1 for alternative splicing outcomes; frameshift btw. exon 2 & 3 are indicated below in **bold and underlined.**

name	Sequence
Halotag	5′-ATG GGC AAA TCC GAC AAA CCA GAC CTG GGT TAT TTC TTC GAC GAC CAC GTC CGC TTC ATG GAT GCC TTC ATC GAA GCC CTG GGT CTG GAA GAG GTC GTC CTG GTC ATT CAC GAC TGG GGC TCC GCT CTG GGT TTC CAC TGG GCC AAG CGC AAT CCA GAG CGC GTC AAA GGT ATT GCA TTT ATG GAG TTC ATC CGC CCT ATC CCG ACC TGG GAC GAA TGG CCA GAA TTT GCC CGC GAG ACC TTC CAG GCC TTC CGC ACC ACC GAC GTC GGC CGC AAG CTG ATC ATC GAT CAG AAC GTT TTT ATC GAG GGT ACG CTG CCG TGG GGT GTC GTC CGC CCG CTG ACT GAA GTC GAG ATG GAC CAT TAC CGC GAG CCG TTC CTG AAT CCT GTT GAC CGC GAG CCA CTG TGG CGC TTC CCA AAC GAG CTG CCA ATC GCC GGT GAG CCA GCG AAC ATC GTC GCG CTG GTC GAA GAA TAC ATG GAC TGG CTG CAC CAG TCC CCT GTC CCG AAG CTG CTG TTC TGG GGC ACC CCA GGC GTT CTG ATC CCA CCG GCC GAA GCC GCT CGC CTG GCC AAA AGC CTG CCT AAC TGC AAG GCT GTG GAC ATC GGC CCG GGT CTG AAT CTG CTG CAA GAA GAC AAC CCG GAC CTG ATC GGC AGC GAG ATC GCG CGC TGG CTG TCT ACT CTG GAG ATT TCC-3′
Linker btw. Halotag & exon 1	5′-TCC GGA CTC AAG ATC T-3′
Exon 1	5′-CC GGA AAT GTT CAG GCT GGA GAC TAT GTG CTA ATC CAT GCA GGA CTG AGT GGT GTG GGC ACA GCT GCT ATC CAA CTC ACC CGG ATG GCT GGA GCT ATT CCT CTG GTC ACA GCT GGC TCC CAG AAG AAG CTT CAA ATG GCA GAA AAG CTT GGA GCA GCT GCT GGA TTC AAT TAC AAA AAA GAG GAT TTC TCT GAA GCA ACG CTG AAA TTC ACC AAA GGT-3′
Exon 2 & exon 3	5′-GCT GGA GTT AAT CTT ATT CTA GAC TGC ATA GGC GGA TCC TAC TGG GAG AAG AAC GTC AAC TGC CTG GCT CTT GAT GGT CGA TGG GTT CTC TAT GGT CTG ATG GGA GGA GGT GAC ATC AAT GGG CCC CTG TTT TCA AAG CTA CTT TTT AAG CGA GGA AGT CTG ATC ACC AGT TTG CTG AGG TCT AGG GAC AAT **AAG** TAC AAG CAA ATG CTG GTG AAT GCT TTC ACG GAG CAA ATT CTG CCT CAC TTC TCC ACG GAG GGC CCC CAA CGT CTG CTG CCG GTT CTG GAC AGA ATC TAC CCA GTG ACC GAA ATC CAG GAG GCC CAT AAG TAC ATG GAG GCC AAC AAG AAC ATA GGC AAG ATC GTC CTG GAA CTG CCC CAG ACG-3′
GFP	5′-ATG AGC GGG GGC GAG GAG CTG TTC GCC GGC ATC GTG CCC GTG CTG ATC GAG CTG GAC GGC GAC GTG CAC GGC CAC AAG TTC AGC GTG CGC GGC GAG GGC GAG GGC GAC GCC GAC TAC GGC AAG CTG GAG ATC AAG TTC ATC TGC ACC ACC GGC AAG CTG CCC GTG CCC TGG CCC ACC CTG GTG ACC ACC CTC TGC TAC GGC ATC CAG TGC TTC GCC CGC TAC CCC GAG CAC ATG AAG ATG AAC GAC TTC TTC AAG AGC GCC ATG CCC GAG GGC TAC ATC CAG GAG CGC ACC ATC CAG TTC CAG GAC GAC GGC AAG TAC AAG ACC CGC GGC GAG GTG AAG TTC GAG GGC GAC ACC CTG GTG AAC CGC ATC GAG CTG AAG GGC AAG GAC TTC AAG GAG GAC GGC AAC ATC CTG GGC CAC AAG CTG GAG TAC AGC TTC AAC AGC CAC AAC

GTG TAC ATC CGC CCC GAC AAG GCC AAC AAC GGC CTG GAG GCT AAC
TTC AAG ACC CGC CAC AAC ATC GAG GGC GGC GGC GTG CAG CTG GCC
GAC CAC TAC CAG ACC AAC GTG CCC CTG GGC GAC GGC CCC GTG CTG
ATC CCC ATC AAC CAC TAC CTG AGC ACT CAG ACC AAG ATC AGC AAG
GAC CGC AAC GAG GCC CGC GAC CAC ATG GTG CTC CTG GAG TCC TTC
AGC GCC TGC TGC CAC ACC CAC GGC ATG GAC GAG CTG TAC AGG
TAA-3′

Supplementary Table 3: Primers used for RNA purification.

Primer	Sequence (5'-3')
Forward - RNA 1a	GGATCCTAATACGACTCACTATAG
Reverse - RNA 1a	GAATTCTCAAGTAATCTGGACGAATTTCAC
Forward - RNA 1b	GGATCCTAATACGACTCACTATAG
Reverse - RNA 1b	GAATTCGAGTCTCCTTGCTCG
Forward - RNA 2a	GGATCCTAATACGACTCACTATAG
Reverse - RNA 2a	GAATTCATCTGGACGAATTTCACG
Forward - RNA 2b	GGATCCTAATACGACTCACTATAG
Reverse - RNA 2b	GAATTCTTGAGTCTCCTTGCT
Forward - RNA 3a	GGATCCTAATACGACTCACTATAG
Reverse - RNA 3a	GAATTCAGTATAACCGTATCAAGTAATCTGGAC
Forward - RNA 3b	GGATCCTAATACGACTCACTATAG
Reverse - RNA 3b	GAATTCGAGTCTCCTTGCTCG
Forward - RNA 2A	GGATCCTAATACGACTCACTATAG
Reverse - RNA 2A	GAATTCATCTGGACGAATTTCACG
Forward - RNA 2B	GGATCCTAATACGACTCACTATAG
Reverse - RNA 2B	GAATTCTTGAGTCTCCTTGCT
Forward - RNA A*	GGATCCTAATACGACTCACTATAG
Reverse - RNA A*	GAATTCTTGAGTCTCCTTGCT

References:

(1) Gurskaya, N. G.; Staroverov, D. B.; Lukyanov, K. A. Chapter Eleven - Fluorescent Protein-Based Quantification of Alternative Splicing of a Target Cassette Exon in Mammalian Cells. In *Methods in Enzymology*; Filonov, G. S., Jaffrey, S. R., Eds.; Academic Press, 2016; Vol. 572, pp 255–268. https://doi.org/10.1016/bs.mie.2016.02.007.

(2) Lu, Z. J.; Gloor, J. W.; Mathews, D. H. Improved RNA Secondary Structure Prediction by Maximizing Expected Pair Accuracy. *RNA* **2009**, *15* (10), 1805–1813. https://doi.org/10.1261/rna.1643609.

(3) Johnson Jr, J. E.; Reyes, F. E.; Polaski, J. T.; Batey, R. T. B12 Cofactors Directly Stabilize an mRNA Regulatory Switch. *Nature* **2012**, *492* (7427), 133–137. https://doi.org/10.1038/nature11607.

(4) Sarfraz, N.; Lee, H. J.; Rice, M. K.; Moscoso, E.; Shafik, L. K.; Glasgow, E.; Ranjit, S.; Lambeck, B. J.; Braselmann, E. Establishing Riboglow-FLIM to Visualize Noncoding RNAs inside Live Zebrafish Embryos. *Biophysical Reports* **2023**, *3* (4), 100132. https://doi.org/10.1016/j.bpr.2023.100132.

(5) Braselmann, E.; Wierzba, A. J.; Polaski, J. T.; Chromiński, M.; Holmes, Z. E.; Hung, S.-T.; Batan, D.; Wheeler, J. R.; Parker, R.; Jimenez, R.; Gryko, D.; Batey, R. T.; Palmer, A. E. A Multicolor Riboswitch-Based Platform for Imaging of RNA in Live Mammalian Cells. *Nature Chemical Biology* **2018**, *14* (10), 964–971. https://doi.org/10.1038/s41589-018-0103-7.

(6) Polaski, J. T.; Webster, S. M.; Johnson, J. E.; Batey, R. T. Cobalamin Riboswitches Exhibit a Broad Range of Ability to Discriminate between Methylcobalamin and Adenosylcobalamin. *Journal of Biological Chemistry* **2017**, *292* (28), 11650–11658. https://doi.org/10.1074/jbc.M117.787176.

(7) Sarfraz, N.; Moscoso, E.; Oertel, T.; Lee, H. J.; Ranjit, S.; Braselmann, E. Visualizing Orthogonal RNAs Simultaneously in Live Mammalian Cells by Fluorescence Lifetime Imaging Microscopy (FLIM). *Nature Communications* **2023**, *14* (1), 867. https://doi.org/10.1038/s41467-023-36531-y.

(8) Frei, M. S.; Tarnawski, M.; Roberti, M. J.; Koch, B.; Hiblot, J.; Johnsson, K. Engineered HaloTag Variants for Fluorescence Lifetime Multiplexing. *Nature Methods* **2022**, *19* (1), 65–70. https://doi.org/10.1038/s41592-021-01341-x.